Protein Cell 2012, 3(6): 470–480
DOI 10.1007/s13238-012-2932-6

Protein & Cell

RESEARCH ARTICLE

Generation of Calhm1 knockout mouse and characterization of calhm1 gene expression

Junbing Wu[1,2], Shengyi Peng[1,2], Rong Wu[1,2], Yumin Hao[1,2], Guangju Ji[1], Zengqiang Yuan[1] ✉

[1] State Key Laboratory of Brain and Cognitive Sciences, Institute of Biophysics, Chinese Academy of Sciences, Beijing 100101, China
[2] College of Life Sciences, Graduate School of Chinese Academy of Sciences, Beijing 100049, China
✉ Correspondence: zqyuan@ibp.ac.cn
Received April 8, 2012 Accepted April 24, 2012

ABSTRACT

Alzheimer's disease (AD) is the most common neurodegenerative disease among elderly people worldwide. Several genes have been validated to be associated with AD, and calcium homeostasis modulator *1* (*Calhm1*) is the latest suspected one. To investigate the biological and pathological function of *Calhm1* systematically, we generated a *Calhm1* conventional knockout mouse. However, both the male and female of elderly *Calhm1* knockout (KO) mice showed similar ability to their wild type littermates in spatial learning and memory retrieving. Surprisingly, we found that *Calhm1* mRNA could not be detected in mouse brains at different ages, although it is expressed in the human brain tissues. We further found that CpG islands (CGIs) of both mouse and human *Calhm1* were hypermethylated, whereas CGI of mouse *Calhm2* was hypomethylated. In addition, transcriptional active marker H3K4Di occupied on promoters of human *Calhm1* and mouse *Calhm2* at a considerable level in brain tissues, while the occupancy of H3K4Di on promoter of mouse *Calhm1* was rare. In sum, we found that mouse *Calhm1* was of rare abundance in brain tissues. So it might not be suitable to utilize the knockout murine model to explore biological function of *Calhm1* in the pathogenesis of AD.

KEYWORDS Alzheimer's disease, calcium homeostasis modulator, methylation, transcription

INTRODUCTION

Alzheimer's disease (AD) is the most common cause of dementia in elderly people worldwide. Advanced aging, family history and heredity are major risk factors of AD. Although the etiology of AD is far more complicated, two pathological hallmarks are common, namely extracellular amyloid plaques depositing of amyloid β (Aβ) and intracellular neurofibriliary tangles (NFT) triggered by hyperphosphorylated tau (Ballard et al., 2011). Genetically, familial mutants of deterministic genes, amyloid precursor protein (APP) on chromosome 21, presenilin 1 (PS1) on chromosome 14 and presenilin 2 (PS2) on chromosome 1, directly cause early-onset AD (EOAD) before age 60, accounting for about 5% of all AD cases (Goate et al., 1991; Levy-Lahad et al., 1995; Sherrington et al., 1995; Tanzi, 1999). In most cases, patients suffer from sporadic AD or late-onset AD (LOAD). It is speculated that many risk genes of relatively low penetrance but high prevalence are associated with LOAD. But only the ε4 allele of apolipoprotein E (ApoE) on chromosome 19 is extensively validated by meta-analysis and is further confirmed by most of the genome-wide association studies (GWAS) in AD patients (Saunders et al., 1993; Farrer et al., 1997; Bertram et al., 2010).

Recently, a novel gene named calcium homeostasis modulator *1* (*Calhm1*) is proposed to be associated with LOAD (Dreses-Werringloer et al., 2008). Human *Calhm1* predominantly expresses in hippocampus and locates on chromosome 10 at 1.6 Mb of the LOAD marker region D10S1671. Calhm1 homomultimerizer forms a multi-pass transmembrane protein, which localizes to plasma membrane and endoplasmic reticulum (ER) and maintains calcium homeostasis. Moreover, a P86L polymorphism of Calhm1 is reported to increase LOAD risk by influencing cytoplasmic calcium oscillation and increasing Aβ levels (Dreses-Werringloer et al., 2008). The conclusion is consistent with the prevalent concept that perturbed calcium homeostasis is

implicated in the pathology of AD. Actually, APP, PS1 and PS2 as well as ApoE have been found to modulate the calcium levels (LaFerla, 2002). However, the results of the follow-up epidemiological studies on the association of Calhm1 mutation with AD are controversial. For instance, in the study of Caucasian American, Japanese, and Belgian, Calhm1 P86L polymorphism is not associated with late-onset AD, while Calhm1 is found to be a risk factor for AD in Chinese population (Beecham et al., 2009; Minster et al., 2009; Sleegers et al., 2009; Boada et al., 2010; Cui et al., 2010; Giedraitis et al., 2010; Inoue et al., 2010; Nacmias et al., 2010; Shibata et al., 2010). In addition, Lambert et al. demonstrates that Calhm1 is not a deterministic gene in the development of AD but may affect the age of onset *via* interacting with *APOE4* gene mutation (Lambert et al., 2010).

Animal models provide an invaluable tool for the study of molecular pathogenesis of AD. Especially, knockout mice greatly facilitate researchers to explore the pathophysiological function of AD-associated genes. For example, APP knockout mice exhibit reduced brain weight, locomotion activity and spatial learning (Zheng et al., 1995). Conventional PS1 knockout mice show developmental deficiency and die shortly after birth (Shen et al., 1997). Conditional knockout PS1 mice in which PS1 is specifically deleted in postnatal forebrain show mild impairment in spatial learning and memory, while PS1 depletion in forebrain impairs the clearance of hippocampal memory traces (Shen et al., 1997; Feng et al., 2001; Yu et al., 2001). Although ApoE knockout mice appear healthy, a line of transgenic mice overexpressing C-terminal truncated ApoE4 display AD-like neurodegeneration (Piedrahita et al., 1992; Harris et al., 2003).

In order to investigate the biological and pathological function of Calhm1 *in vivo*, we generated a Calhm1 conventional knockout mouse model. Calhm1 knockout mice could survive for at least 18 months, grew normally as WT littermates, and exhibited similar spatial learning and memory ability comparing with WT mice when probed in Morris water maze task. Furthermore, we found that *Calhm1* mRNA in mouse brains of different ages could not be detected by regular biochemical experiments such as absolute quantitative RT-PCR, indicating there is a very low expression level of *Calhm1* in mouse. In other experiments, we found that CpG islands (CGIs) in the promoter and first exon of both mouse and human *Calhm1* were hypermethylated, compared with hypomethylated status of mouse *Calhm2* gene. We also observed that the transcriptional active marker H3K4Di (histone H3 lysine 4 dimethylation) rarely occupied on the promoter of mouse *Calhm1*, but occupied on that of human *Calhm1* and mouse *Calhm2* at a considerable level in brain tissues. In addition, we found that *Calhm1* genomic depletion does not affect the expression of *Calhm2* in mouse brains. Taken together, it may not be suitable to study the physiology function of Calhm1 in knockout mouse model.

RESULTS

Generation of *Calhm1* conventional knockout mice

The Calhm (Calcium homeostasis modulator) family genes consist of three members that are clustered in the chromosome 19. The mouse *Calhm1* contains two exons, which is located in the locus between *Calhm2* and *Calhm3* loci without overlapping. We employed the strategy of replacing the two exons and the intron in between with a PGK-neo cassette (Fig. 1A). The Calhm1 gene targeting vector was constructed by lambda (λ) Red-mediated recombineering in *Escherichia coli.* (Liu et al., 2003). The genomic sequence containing Calhm1 genome and the flanking recombination arms was retrieved from 129Sv bacterial artificial chromosome (BAC) clone. Then two exons and one intron in *Calhm1* were replaced with a neomycin cassette driven by PGK promoter. Linearized construct was electroporated into mouse embryonic stem (ES) cells. 7 of 48 ES colonies were screened out by 5'- and 3'-long-amplicon PCR (Fig. 1B). Correct homologous recombination events were further confirmed by Southern blotting (Fig. 1C). Two positive clones of them were microinjected into C57/B6 blastocysts separately, and were transplanted into pseudopregnant mice. Chimeric progenies were backcrossed with C57/B6 mice to generate F1 offsprings. Genotyping of F1 generation revealed that heterozygous Calhm1 mice were available, confirming that the germ line transmission was normal. All those evidences indicated the generation of Calhm1 conventional knockout mouse model was successful.

Calhm1 KO mice were generated by intercross of heterozygous Calhm1 mice and confirmed by genotyping (Fig. 1D). The progeny of Calhm1 mice exhibited normal Mendelian ratios, and both male and female Calhm1 KO mice were fertile. Calhm1 KO mice grew normally compared to their WT littermates, even at an elder age of 18 months.

Examination of learning and memory ability of Calhm1 KO mice

Human *Calhm1* mRNA was detected in hippocampus in adult brain but not in the fetal brain, and was supposed to be associated with LOAD. In order to characterize whether there are cognitive declines in Calhm1 knockout mice, we performed the Morris water maze test. Paired mice were grouped by gender and genotype. During the 10 days trail, the spatial learning ability of Calhm1 WT and KO mice, which was indicated by the latency to reach the platform, showed no significant difference in both genders (Fig. 2A and 2B). Moreover, both WT and KO mice of both genders displayed similar retrieving memory on the quadrant preference (Fig. 2C and 2D). The latency to position of platform in the probe was also not significantly different between WT and KO mice (Fig. 2E and 2F). In addition, weights of those mice were comparable (Fig. 2G and 2H). Taken together, we concluded

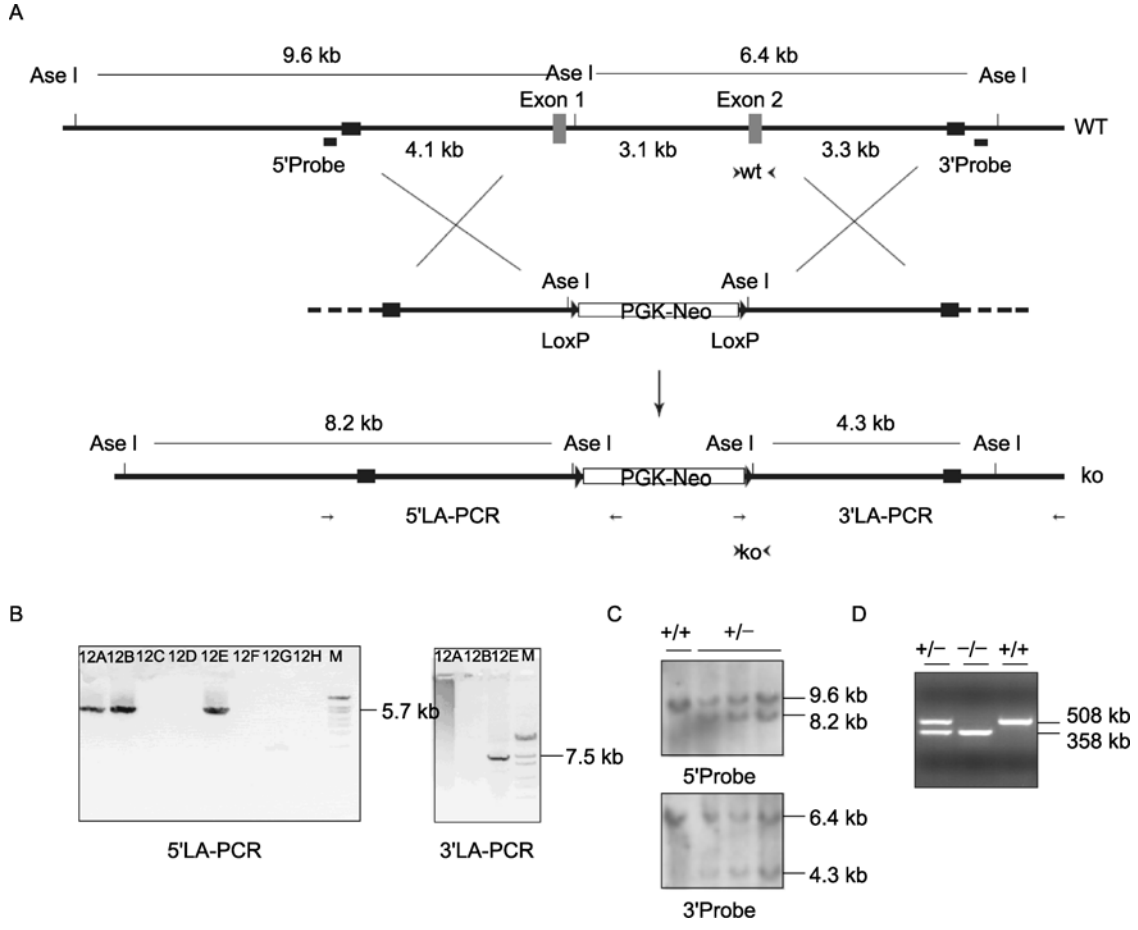

Figure 1. Generation of Calhm1 conventional knockout mice. (A) The knockout strategy of Calhm1. About 3.1-kb long genomic sequences, including two exons and the flanked intron of *Calhm1* locus, is replaced by a PGK promoter-driving neomycin cassette (PGK-Neo). The 5' arm and 3' arm for recombination in ES cells is 4.1 kb and 3.3 kb respectively. (B) Long amplicon PCR (LA-PCR) screening of ES clones. One primer of each pair located in WT genome and the other located in PGK-Neo Cassette, flanking the recombination arm completely. Positive clones of 5' terminal and 3' terminal LA-PCR are 5.7 kb and 7.5 kb long, respectively. (C) Southern blot confirmation of PCR positive ES Cell clones. The genomic DNA is digested with AseI, and then hybridized with 5' probe and 3' probe separately. WT control, 5' terminal, 9.6 kb only; 3' terminal, 6.4 kb only. Positive clones, 5' terminal, 9.6 kb and 8.2 kb; 3' terminal, 6.4 kb and 4.3 kb. (D) Genotyping of offspring bred by intercross of Calhm1 heterozygous mice. +/+, 508 bp only; +/-, 508 bp and 358 bp; -/-, 358 bp only.

that Calhm1 KO mice showed no cognitive decline in the task.

Calhm1 was not expressed in mouse brains

The findings of no learning and memory deficiency in the Calhm1 KO mice led us to examine the spatiotemporal expression pattern of *Calhm1* in the mouse brain at different ages (postnatal day 7 (P7), P14, P30, 2-month, 6-month). We could not detect the specific signals in the brain sections by RNA *in situ* hybridization (data not shown).

Previous study showed that human *Calhm1* could be detected in human brain samples by RT-PCR (Dreses-Werringloer et al., 2008), which is also confirmed in our study (Fig. 3A). However, there was no report of *Calhm1* expression in mice. Actually, we could not detect the *Calhm1* expression by RT-PCR in our experiments (data not shown). In comparison, several low abundant genes in mouse brains, such as *TRPC2*, *TRPM4* and *TRPV1*, could be detected by RT-PCR (Fig. 3B) (Kunert-Keil et al., 2006). Those experiments raised the possibility that mouse *Calhm1* might be expressed at a very low level in mouse brains, whereas human *Calhm1* was expressed in human brains.

To examine the expression of mouse *Calhm1* more thoroughly, absolute real-time reverse transcription PCR was performed to evaluate Calhm1 mRNA level of mouse brains at different ages (Dreses-Werringloer et al., 2008). Considering the comparable complexity of transcriptome and genome,

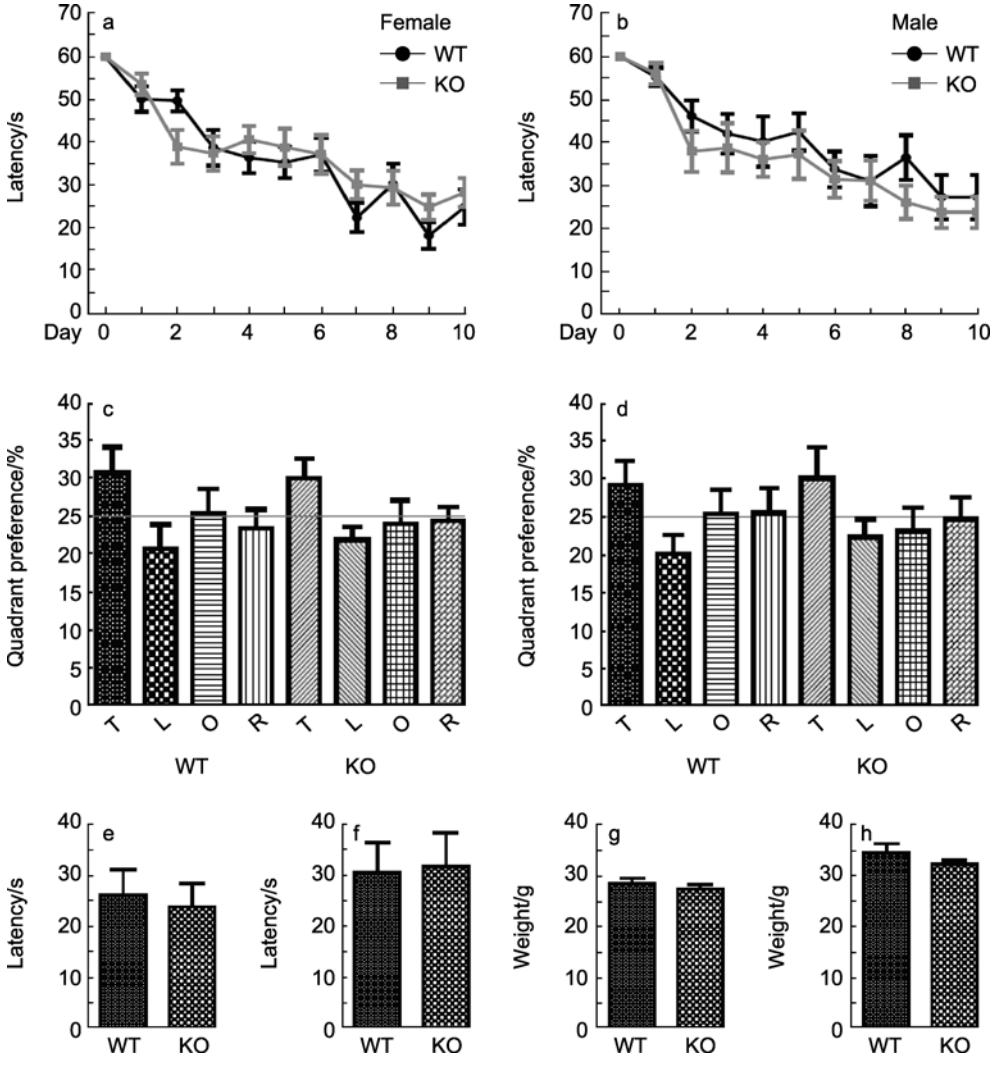

Figure 2. Morris Water Maze test of *Calhm1* WT and KO mice. (A and B) Learning curves of Calhm1 female and male mice per day in the trial, respectively. A 10-day and 2 trials per day learning were performed, and the latency to the target was plotted with the days. Female group, WT, $n = 16$, KO, $n = 16$; Two-way ANOVA, P value of time < 0.001; P value of genotype = 0.3548, no significant difference. Male group, WT, $n = 10$, KO, $n = 12$; Two-way ANOVA, P value of time < 0.001; P value of genotype = 0.9403, no significant difference. (C, D) Quadrant preference of Calhm1 knockout mice in 1 min probe at day 11. T, target quadrant; O, opposite quadrant; L, left quadrant; R, right quadrant. Female group, WT and KO, T versus L, unpaired t-test, $P < 0.05$; Male group, WT, T versus L, unpaired t-test, $P < 0.05$. (E and F) Latency to target of Calhm1 female and male mice in 1 min probe at day 11. Female group, WT versus KO, unpaired t-test, $P = 0.7470$, no significant difference. Male group, WT versus KO, unpaired t-test, $P = 0.9003$, no significant difference. (G and H) Body weights of Calhm1 WT and KO mice in the task. Female group, WT versus KO, unpaired t-test, $P = 0.4290$, no significant difference. Male group, WT versus KO, unpaired t-test, $P = 0.2450$, no significant difference.

genomic DNA is more suitable to be taken as standards in absolute quantification real-time RT-PCR. Since a whole haploid mouse genome contains approximate 3 pg, we equaled 3 pg of genomic DNA to a single copy of genes (Laird, 1971). Each PCR amplicon is located in an exon, so that primer sets could be used to amplify both genomic DNA and cDNA. RNAs were treated with DNase I to eliminate genomic contamination in the transcripted cDNA. Taqman probe based method was adopted to guarantee specific quantification of amplicons even in trace abundance. The method was first verified by quantifying β-actin mRNA (Fig. 3C). Then, *Calhm1* and *Calhm2* mRNA from mouse brains of embryonic day 14 (E14), E16 and E18, postnatal day 0 (P0), P7, P14, 2-week-old, 4-week-old, 4-month-old, 8-month-old and 1-year-old, was quantified simultaneously. The results demonstrated that *Calhm2* mRNA expressed at a considerable level whereas *Calhm1* mRNA was undetectable at all age brains (Fig. 3D).

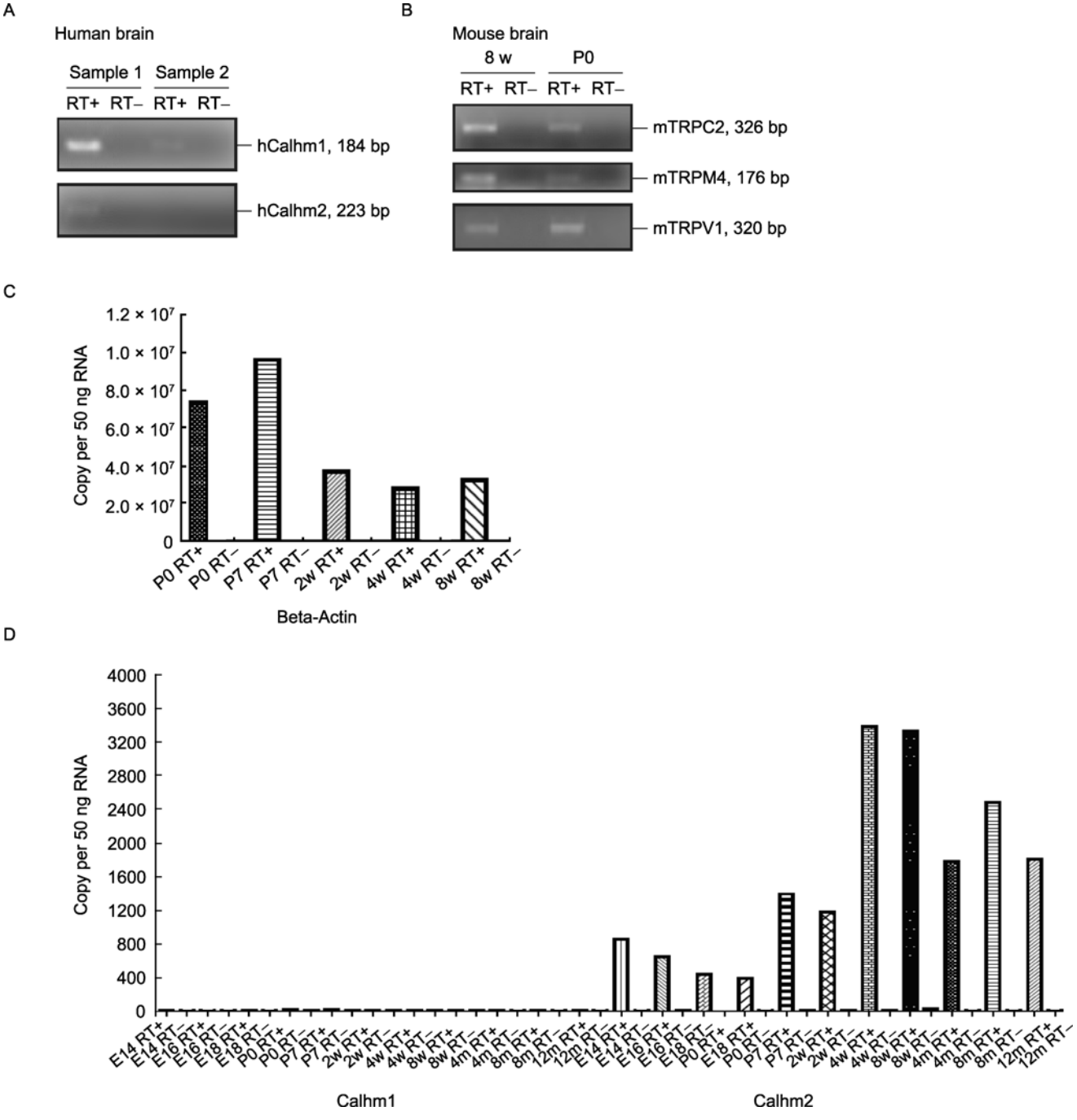

Figure 3. Expression of Calhm1 and Calhm2 mRNA. (A) Expression of Calhm1 and Calhm2 mRNA in human brain samples. (B) Expression of low abundance genes in mouse brain samples. (C) Absolute quantification of beta-actin mRNA in mouse brain. (D) Absolute quantification of Calhm1 and Calhm2 mRNA in mouse brain samples at different age stages by real-time qRT-PCR. E14, embryonic day 14; P0, postnatal day 0; 8w, 8 weeks old; 12m, 12 months old; RT+, normal reverse transcription; RT-, RT control without reverse transcriptase. A typical result of two independent experiments was demonstrated.

CpG islands of *Calhm1* were hypermethylated

DNA methylation and histone modifications are supposed to collaborate to repress gene transcription in the long term manner (Fuks, 2005). So we attempted to check the status of epigenetic marks to explain the discrepancy between mouse and human *Calhm1* genes.

CpG islands (CGIs) of promoter and exon 1 were pre-

dicted by MSP primer program followed criteria as, (a) at least 200 bp length, (b) CG content > 50%, and (c) the ratio of observed CpG content *versus* expected CpG content > 0.6 (Brandes et al., 2007). All CGIs of mouse *Calhm1*, mouse *Calhm2* and human *Calhm1* located in downstream of transcription start site (TSS). Bisulfate sequencing results demonstrated that CGIs of both mouse and human *Calhm1* were hypermethylated (94.07% and 93.04%), while CGI of mouse *Calhm2* was hypomethylated (15.74%) (Fig. 4A–4D).

The active epigenetic mark rarely occupies on promoter of mouse Calhm1

The promoters were further investigated by native chromatin immunoprecipitation (NChIP) with anti-H3K4Di antibody, which was generally considered as an active marker of transcription. ChIP/Input ratios indicated that H3K4Di occupied on the promoter of human *Calhm1* and the promoter of mouse *Calhm2* at a considerable level in brain tissues, whereas H3K4Di occupancy on mouse *Calhm1* was close to the IgG background (Fig. 5A–5C). Both CGI methylation and H3K4 modification indicated that the transcription of mouse *Calhm1* was inactive, which was consistent with RT-PCR results (Fig. 3D).

Genomic locus of mouse *Calhm2* is in the downstream of *Calhm1*. To exclude the possibility that deletion of *Calhm1* locus might affect the expression of *Calhm2* mRNA, *Calhm2* mRNA level of 6 paired littermates of *Calhm1* WT and KO mice was measured. The result revealed that *Calhm2* mRNA levels of mouse brains were not affected by *Calhm1* depletion (Fig. 5D).

DISCUSSION

Knockout mice are invaluable models for the study of AD pathogenesis. In this study, we had successfully generated a Calhm1 conventional knockout mouse. Calhm1 KO mice developed and matured normally and showed no obvious cognitive decline till one-year old age. Human *Calhm1* mRNA was expressed in human brains and tongues (Dreses-Werringloer et al., 2008; Moyer et al., 2009), while we found that mouse Calhm1 mRNA was of rare abundance in mouse brains. When blasted with NCBI EST databases (Zhang et al., 2000), there were above 100 hints of human *Calhm1* mRNA but none of mouse *Calhm1* mRNA (blast subjected on March 26, 2012). Query of mouse Calhm1 on gene expression omnibus (GEO), a high-throughput database (Edgar et al., 2002), showed only 7 records and none of them was analyzed of

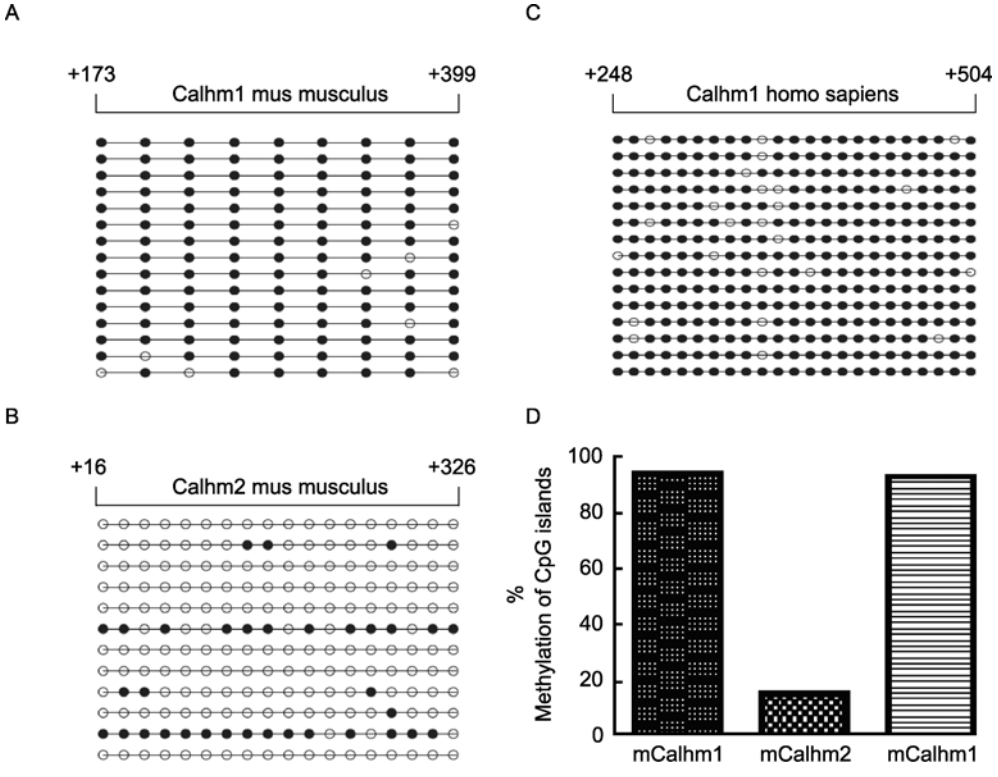

Figure 4. Methylation of CpG islands in the predicted promoter and/or exon 1 of Calhm1 and Calhm2. (A and B) CGI methylation of Calhm1 and Calhm2 in mouse brain samples was demonstrated by bisulfate genomic sequencing, respectively. (C) CGI methylation of Calhm1 in human brain samples. Solid and circular dots indicated methylated and unmethylated CpG sites, respectively. TSS, transcription start site. (D) Summary of the percentage of CGI methylation (mCalhm1, 94.07%; mCalhm2, 15.74%; hCalhm1, 93.04%).

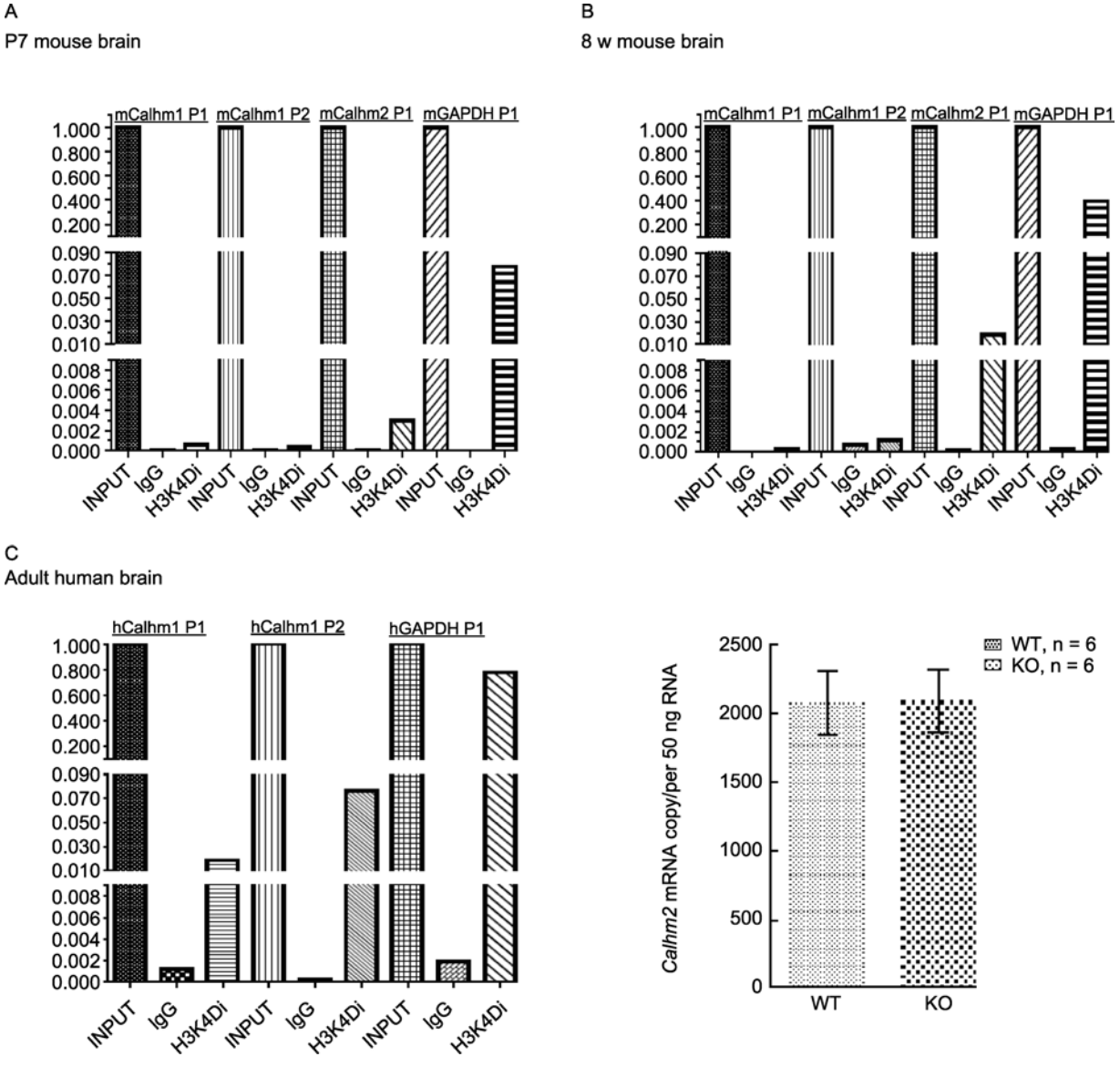

Figure 5. Transcriptional activity of the predicted promoter of *Calhm1* and *Calhm2*. (A and B) Transcriptional active marker H3K4Di occupancy on the promoter of *Calhm1* and *Calhm2* in mouse brain samples. ChIP/input ratio, 7 d, Calhm1, 0.05% and 0.04%, Calhm2, 0.29%, GAPDH, 7.78%; 8w, Calhm1, 0.03% and 0.11% (background 0.08%), Calhm2, 1.87%, GAPDH, 39.42%. (C) H3K4Di occupancy on the promoter of Calhm1 in human brain sample. ChIP/input ratio, Calhm1, 1.18% and 7.62%, GAPDH, 77.84%. Native chromatin was immunoprecipitated by anti-H3K4Di antibody, and genomic region of the promoter was amplified with corresponding primers by semi-quantitative PCR. Promoters of GAPDH were taken as positive control. (D) Calhm1 locus depletion didn't affect the expression of *Calhm2* mRNA in mouse brain. mRNA of six paired littermates of Calhm1 WT and KO mice, 10–13 months old, was quantified by real-time qRT-PCR. WT versus KO, 2075 ± 232.0 versus 2088 ± 229.4, unpaired t-test, *P* value = 0.9684, no significant difference, *n* = 6.

brain tissues (query subjected on March 26, 2012). Those bioinformatic data further supported our absolute quantification of mouse *Calhm1* mRNA.

In mammals, promoters were usually associated with CGIs, which were equipped to regulate gene activity (Deaton and Bird, 2011). Unlike the consistency of CGI methylation and histone modification of mouse *Calhm1*, mouse *Calhm2* and housekeeping genes, CGI of human *Calhm1* was hypermethylated, but transcriptional active marker H3K4Di occupancy on promoter was of a considerable level. Such difference between human and mouse *Calhm1* may explain the reason why human *Calhm1* expressed but mouse *Calhm1* didn't. Although we have not clarified mechanisms that caused the discrepancy completely, we had provided a clue

for further investigation.

Finally, since mouse *Calhm1* is unlikely expressed and mouse *Calhm3* is a pseudogene, mouse *Calhm2* may function redundantly for the Calhm family genes. It may be interesting to generate the Calhm2 knockout mice as the murine models to study the role and molecular mechanism of CALHM family proteins in the pathogenesis of Alzheimer's diseases in the future.

MATERIALS AND METHODS

Animals

All experiments of animals followed guidelines from Administration Regulations on Laboratory Animals of Beijing. The use of human brain samples for investigation was approved by the Medical Science Ethics Committee of Chinese PLA General Hospital.

Generation of knockout mouse

The targeting construct of Calhm1 conventional knockout was generated via bacteriophage-based recombineering system in *E. coli* (Liu et al., 2003). Genomic region from 4.1 kb upstream to 3.1 kb downstream of Calhm1 locus, was retrieved from BAC (BAC No., bMQ71e17) to pL253 plasmid via homologous recombination in EL350. Then genomic region of Calhm1 including two exons and the intron in-between was replaced by a 2.1 Kb long cassette loxP-neo-loxP *via* homologous recombination in EL350 similarly. Linearized construct was electroporated into 129Sv mouse embryonic stem (ES) cells by Gene Pulser (Bio-Rad), and then was selected by G418 (Sigma) and ganciclovir (GCV) (Sigma). Drug resistant ES colonies were incubated in lysis buffer (10 mmol/L Tris/HCl, pH 7.5, 10 mmol/L EDTA, 10 mmol/L NaCl, 0.5% Sarcosyl (Sigma), 1 mg/mL Proteinase K) and genomic DNA was prepared through phenol/chloroform extraction method. Positive colonies were screened out by long-amplicon PCR (LA-PCR) and followed by Southern blotting.

LA-PCR was performed for both 5' and 3' terminals separately. One primer of LA-PCR located in WT genome and the other located in PGK-Neo Cassette, spanning the recombination arm completely. 5' LA-PCR was performed by LA Taq (TaKaRa) following the program, 94°C, 30s; 63°C, 30s; 68°C, 6 min, 40 cycles, and the product size of which was 5690 bp. Primers of 5' LA-PCR were, C1-ES5T-F, 5'-ggg cag tca cac aac aca cag taa-3', and C1-ES5T-R, 5'-ccg aat agc ctc tcc acc caa gcg-3'. 3' LA-PCR was performed following the program, 94°C, 30s; 61.9°C, 30s; 68°C, 8 min, 40 cycles, and the product size of which was 7542 bp. Primers of 3' LA-PCR were, C1-ES3T-F, 5'-gcc act ccc act gtc ctt tcc ta-3', and C1-ES3T-2R, 5'-gcc ctc tct gcc tac tgc ttg t-3'. Only the colonies with both positive PCR products were subjected to further confirmation by Southern blot.

Southern blot was performed as described in a handbook (Sambrook and Russell, 2001). In brief, 10 μg Genomic DNA was digested with AseI (NEB labs), separated by agarose gel electrophoresis, transferred onto Hybond-N nylon membrane (GE Healthcare). After crosslink with ultraviolet (UVP Ultraviolet Crosslinkers), membranes were hybridized with 5' and 3' probes in Rapid-Hyb buffer, respectively (GE healthcare). Probes were amplified by rTaq and were incorporated with radioactive ^{32}P using Rediprime II random prime labelling system (GE healthcare) and α-[^{32}P]-dCTP (PerkinElmer). The blots were finally developed by autoradiograph.

Several positive ES colonies were microinjected into C57/B6L blastocysts and transplanted into pseduopregnant mice. When the offspring matured, the chimeric ones were backcrossed to C57/B6L mice to generate the F1 progeny.

Genotyping

About 5 mm-long mouse tails were obtained and were incubated in 500 μL tail lysis buffer (100 mmol/L Tris/HCl, pH 8.0, 5 mmol/L EDTA, 0.2% SDS, 200 mmol/L NaCl, 400 μg/mL Proteinase K) at 50°C overnight. After centrifugation at 14,000 rpm for 10 min, the supernatant were transferred to new Eppendorf tubes and mixed with 500 μL isopropanol. Genomic DNA pellets were precipitated after a second centrifugation. Once washed with 70% ethanol, the pellets were dried by a vacuum (Labconco) and were dissolved in 100 μL double distilled water. Genotyping through multiplex PCR was performed with 2 μL genomic DNA and three primers (Calhm1-gtWTF2, 5'-tcc ctc gga cag gac aga aga aga-3', Calhm1-gtKOF2, 5'-gcc act ccc act gtc ctt tcc ta-3', and Calhm1-gtWTR2, 5'-ggg atg gaa cga aca gta tca gga-3'). PCR products were resolved through 2% agarose electrophoresis. The product size of WT allele and KO allele was 508 bp and 358 bp, respectively.

Morris water maze test

MWM test was performed following the protocol described with minor modification (Vorhees and Williams, 2006). WT and KO mice were generated by crossing heterozygous male with heterozygous female consecutively for 4 generations. 11–13 months old F4 progeny were classified to female group and male group. Each group contained WT and KO genotype. One day before the trial, the mice were released into a 122-mm diameter tank to swim for 1 min. Learning trails were carried out for 10 consecutive days, with 2 trails per day. In every trail, mice were limited to reach the platform in 1 min, and then were left on the platform for 15 s. Probe was conducted 24 h later after last trail of the whole learning process. Platform was removed, and mice were allowed to retrieve the position of platform for 1 min. Mice were tracked by a video camera (Sony) in both trails and probe. Collected data were analyzed by SMART 2.5 software (Panlab, Harvard Apparatus).

Absolute quantitative real-time PCR

Brain samples were homogenized in TRIzol (Life Technologies) using Bio-Gen PRO200 (PRO Scientific Inc). Total RNA was isolated following the instruction and treated with DNase (TURBO DNA-free Kit, Ambion) to eliminate contaminating genomic DNA. Qualified RNA was quantified by Nanodrop 2000 (Thermo) and 1μg RNA was reverse transcripted by PrimeScript RT kit (TakaRa), which had been optimized for real-time RT-PCR. Absolute quantification through Taqman probe based real-time RT-PCR was performed with Premix Ex Taq Perfect Real Time Kit (TaKaRa) on ABI7300 (Applied Bio-

systems). The primer and probe sets were designed by Primer Express 3.0 Software (Applied Biosystems) and were purchased from Life Technologies. Quantified and six consecutive serial diluted genomic DNA was applied to plot standard curves and double distilled water was used as no template control (NTC) in the absolute quantitative real-time PCR. Each sample including standard and NTC were replicated 5-6 times in a batch. Primer sets were listed as follows, β-actin-quant-F, 5'-ACG GCC AGG TCA TCA CTA TTG-3', β-Actin-quant-R, 5'-CAA GAA GGA AGG CTG GAA AAG A-3' and β-Actin-quant-Probe, 5'-FAM-CAA CGA GCG GTT CCG ATG CCC T-TRAMA-3'; Calhm1- quant-F, 5'-CCA TGC TAG CTG AAG AGT GGA A-3', Calhm1-quant-R, 5'-GGA ACA GAA CAT GTA GCG TAG AAC A-3', and Calhm1-quant-Probe, 5'-FAM- TCG CCG GGC CAA GGA CCC-TRAMA-3'; Calhm2-quant-F, 5'-CCT GAC CAA GTG CCT CAA ACA-3', Calhm2-quant-R, 5'-GGT CCT CGT TGG TAC GGT ACT G-3', and Calhm2-quant-Probe, 5'-FAM-TAC TGC TCG CCA CTC AGC TAC CGT CA-TRAMA-3'.

Bisulfate sequencing

Bisulfate sequencing was performed as described (Coffee, 2009). Genomic DNA from brain samples was prepared using Wizard Genomic DNA Purification Kit (Promega). Up to 1 μg genomic DNA was reconstituted in 25 μL double distilled water and was denatured with 2.75 μL of 2 mol/L NaOH at 37°C for 10 min. The solution was then combined with 15 μL of 10 mmol/L hydroquinone (Sigma) and 260 μL of 3.6 mmol/L sodium bisulfate (Sigma), covered by mineral oil, and was incubated at 54°C for 16 h. The sulfonated DNA was further purified through Wizard DNA Clean-Up System (Promega), reconstituted in 50 μL distilled water, and was incubated with 5.5 μL of 3 mmol/L NaOH at room temperature for 5 min. The single strand DNA was purified through ethanol precipitation method and was amplified by high-fidelity Taq (CWBio). The PCR product was ligated into pEASY-T1 vector (Transgen) for blue/white colony screening. White colonies from 2 mouse samples and 2 human samples were sent for sequencing. The genomic region from 2 kb upstream TSS to first exon of Calhm1 and Calhm2 locus were analyzed and CpG islands were predicted by MSPprimer program (Brandes et al., 2007). The primer sets were listed below, mCalhm1-BiSeq-F, 5'-GGT TTA TAG TTT GGG TAT ATT GTT GA-3' and mCalhm1-BiSeq-R, 5'-CAA ACT ACC ATT ACC TAA TAT AAC C-3', mCalhm2-BiSeq-F, 5'-CAC TTC CTC TAT TTC TAC CTC-3' and mCalhm2-BiSeq-R, 5'-TTT TGG ATT TTT GAT GGA TTG ATA GT-3', hCalhm1-BiSeq-F, 5'-TCT TCC AAT TCC TAC AAT CCA A-3' and hCalhm1-BiSeq-R, 5'-TGT AGA AGG TAT AGA GGA AGT ATT T-3'. All reagents in this experiment were purchased from Sigma and were prepared for fresh use.

Native chromatin immunoprecipitation (NChIP)

NChIP was performed as described previously (Matevossian and Akbarian, 2008). 50–500 mg of snap frozen brain tissue was homogenized in douncing buffer (10 mmol/L Tris/HCl, pH 7.5, 4 mmol/L $MgCl_2$, 1 mmol/L $CaCl_2$) with cocktail protease inhibitor (Roche) by homogenizer dounce (Wheaton). The lysate was incubated with 5 U/mL micrococcal nuclease (NEBiolabs) at 37°C for 7 min and the reaction was quenched immediately by EDTA at a final concentration of 10 mmol/L. After pre-clear with 100 μL Salmon sperm DNA-conjugated Protein G agarose (Millipore) at room temperature for 30 min, and after a brief spin down, 500 μL of the supernatant was aliquot as inputs and 1.6 mL as ChIP samples. After equilibrium with 1/10 volume of 10 × FSB (50 mmol/L EDTA, 200 mmol/L Tris/HCl, pH 7.5, 500 mmol/L NaCl), each ChIP sample was incubated with 3 μg anti-H3K4Di (Abcam) overnight at 4°C. Next day, each ChIP sample was mixed with 50 μL Salmon sperm DNA-conjugated protein G agarose and was rotated at 4°C for another 3 hours. After centrifugation, the pellets were sequentially washed with low salt washing buffer (0.1% SDS, 1% Triton X-100, 2 mmol/L EDTA, 20 mmol/L Tris/HCl, pH 8.0, 150 mmol/L NaCl), high salt washing buffer (0.1% SDS, 1% Triton X-100, 2 mmol/L EDTA, 20 mmol/L Tris/HCl, pH 8.0, 500 mmol/L NaCl), LiCl buffer, and TE buffer (10 mmol/L Tris/HCl, 1 mmol/L EDTA, pH 8.0). Then the pellet was eluted twice with 250 μL elution buffer (0.1 M $NaHCO_3$, 1% SDS). Both input samples and ChIP samples were digested in 50 μg/mL proteinase K at 52°C for 3 hours. DNA was purified using phenol/chloroform method with Glycoblue (Ambion) as a carrier. Dissolved DNA was amplified by SYBR Green based Realtime PCR (Corrbette 6000). The ratios of ChIP versus Input were analyzed. PCR primers are designed by Prime3 program (Rozen and Skaletsky, 2000). Primers used in this experiment were listed below, mCalhm1-Prom-1F, 5'-CCT CTC TGC CAG CAC CTG TT-3' and mCalhm1-Prom-1R, 5'-CCC ACT AGG CAT CCA CCT CA-3', mCalhm1-Prom-2F, 5'-TTG TAA TGC CTG CCC CTC TG-3', and mCalhm1- Prom-2R, 5'-GGA AAT GAT GGC GGT GCT AA-3', mCalhm2-Prom-1F, 5'-CAC GGG TAC CGA TTG CTC TC-3' and mCalhm2-Promot-1R, 5'-GCT GGG ACA GTG GGA TTC AC-3', mGAPDH-Prom-1F, 5'-GCA GGG CAT CCT GAC CTA TG-3' and mGAPDH-Prom-1R, 5'-CTT GTG TAC CGC GCT GTG AG-3', hCalhm1- Prom-1F, 5'-ACA CAG GCA GGC TGA CAC AA-3' and hCalhm1-Prom-1R, 5'-TGT GGA CGT GGC GTA GAA TG-3', hCalhm1-Prom-2F, 5'-GTC ATC GGG GAA CTG ATG GA-3' and hCalhm1-Prom-2R, 5'-GAA GCT CAT CGC CCT CCT TT-3', hGAPDH-Prom-1F, 5'-CCA ATT CCC CAT CTC AGT CG-3' and hGAPDH-Prom-1R, 5'-GAG GTG ATC GGT GCT GGT TC-3'.

Statistical analysis

All data were analyzed using software Graphpad Prism. The column and bar denoted Mean ± SEM.

ACKNOWLEDGMENTS

This work was supported by the National Basic Research Program (973 Program) (Grant No. 2009CB918704) and the National Natural Science Foundation of China (Grant Nos. 81125010 and 81030025). Human tissue was provided by Chinese PLA General Hospital. Calhm1 knockout mouse was generated at Model Animal Research Center of Nanjing University. Thank Dr. Fuchou Tang from Peking University for the help of the absolute real-time RT-PCR.

ABBREVIATIONS

AD, Alzheimer's disease; Calhm1, Calcium homeostatisis modulator 1; CGI, CpG island; ESC, embryonic stem cell; KO, knockout; WT, wild type

REFERENCES

Ballard, C., Gauthier, S., Corbett, A., Brayne, C., Aarsland, D., and Jones, E. (2011). Alzheimer's disease. Lancet 377, 1019–1031.

Beecham, G.W., SchnetzBoutaud, N., Haines, J.L., and PericakVance, M.A. (2009). CALHM1 polymorphism is not associated with late-onset Alzheimer disease. Ann Hum Genet 73, 379–381.

Bertram, L., Lill, C.M., and Tanzi, R.E. (2010). The genetics of Alzheimer disease: back to the future. Neuron 68, 270–281.

Boada, M., Antunez, C., Lopez-Arrieta, J., Galan, J.J., Moron, F.J., Hernandez, I., Marin, J., Martinez-Lage, P., Alegret, M., Carrasco, J.M., et al. (2010). CALHM1 P86L polymorphism is associated with late-onset Alzheimer's disease in a recessive model. J Alzheimers Dis 20, 247–251.

Brandes, J.C., Carraway, H., and Herman, J.G. (2007). Optimal primer design using the novel primer design program: MSPprimer provides accurate methylation analysis of the ATM promoter. Oncogene 26, 6229–6237.

Coffee, B. (2009). Methylation-specific PCR. Curr Protoc Hum Genet Chapter 10, Unit 10 16.

Cui, P.J., Zheng, L., Cao, L., Wang, Y., Deng, Y.L., Wang, G., Xu, W., Tang, H.D., Ma, J.F., Zhang, T., et al. (2010). CALHM1 P86L polymorphism is a risk factor for Alzheimer's disease in the Chinese population. J Alzheimers Dis 19, 31–35.

Deaton, A.M., and Bird, A. (2011). CpG islands and the regulation of transcription. Genes Dev 25, 1010–1022.

Dreses-Werringloer, U., Lambert, J.C., Vingtdeux, V., Zhao, H., Vais, H., Siebert, A., Jain, A., Koppel, J., Rovelet-Lecrux, A., Hannequin, D., et al. (2008). A polymorphism in CALHM1 influences Ca2+ homeostasis, Abeta levels, and Alzheimer's disease risk. Cell 133, 1149–1161.

Edgar, R., Domrachev, M., and Lash, A.E. (2002). Gene Expression Omnibus: NCBI gene expression and hybridization array data repository. Nucleic acids research 30, 207–210.

Farrer, L.A., Cupples, L.A., Haines, J.L., Hyman, B., Kukull, W.A., Mayeux, R., Myers, R.H., Pericak-Vance, M.A., Risch, N., and van Duijn, C.M. (1997). Effects of age, sex, and ethnicity on the association between apolipoprotein E genotype and Alzheimer disease. A meta-analysis. APOE and Alzheimer Disease Meta Analysis Consortium. JAMA 278, 1349–1356.

Feng, R., Rampon, C., Tang, Y.P., Shrom, D., Jin, J., Kyin, M., Sopher, B., Miller, M.W., Ware, C.B., Martin, G.M., et al. (2001). Deficient neurogenesis in forebrain-specific presenilin-1 knockout mice is associated with reduced clearance of hippocampal memory traces. Neuron 32, 911–926.

Fuks, F. (2005). DNA methylation and histone modifications: teaming up to silence genes. Curr Opin Genet Dev 15, 490–495.

Giedraitis, V., Glaser, A., Sarajarvi, T., Brundin, R., Gunnarsson, M.D., Schjeide, B.M., Tanzi, R.E., Helisalmi, S., Pirttila, T., Kilander, L., et al. (2010). CALHM1 P86L polymorphism does not alter amyloid-beta or tau in cerebrospinal fluid. Neurosci Lett 469, 265–267.

Goate, A., Chartier-Harlin, M.C., Mullan, M., Brown, J., Crawford, F., Fidani, L., Giuffra, L., Haynes, A., Irving, N., James, L., et al. (1991). Segregation of a missense mutation in the amyloid precursor protein gene with familial Alzheimer's disease. Nature 349, 704–706.

Harris, F.M., Brecht, W.J., Xu, Q., Tesseur, I., Kekonius, L., Wyss-Coray, T., Fish, J.D., Masliah, E., Hopkins, P.C., Scearce-Levie, K., et al. (2003). Carboxyl-terminal-truncated apolipoprotein E4 causes Alzheimer's disease-like neurodegeneration and behavioral deficits in transgenic mice. Proc Natl Acad Sci U S A 100, 10966–10971.

Inoue, K., Tanaka, N., Yamashita, F., Sawano, Y., Asada, T., and Goto, Y. (2010). The P86L common allele of CALHM1 does not influence risk for Alzheimer disease in Japanese cohorts. Am J Med Genet B Neuropsychiatr Genet 153B, 532–535.

Kunert-Keil, C., Bisping, F., Kruger, J., and Brinkmeier, H. (2006). Tissue-specific expression of TRP channel genes in the mouse and its variation in three different mouse strains. BMC Genomics 7, 159.

LaFerla, F.M. (2002). Calcium dyshomeostasis and intracellular signalling in Alzheimer's disease. Nat Rev Neurosci 3, 862–872.

Laird, C.D. (1971). Chromatid structure: relationship between DNA content and nucleotide sequence diversity. Chromosoma 32, 378–406.

Lambert, J.C., Sleegers, K., Gonzalez-Perez, A., Ingelsson, M., Beecham, G.W., Hiltunen, M., Combarros, O., Bullido, M.J., Brouwers, N., Bettens, K., et al. (2010). The CALHM1 P86L polymorphism is a genetic modifier of age at onset in Alzheimer's disease: a meta-analysis study. J Alzheimers Dis 22, 247–255.

Levy-Lahad, E., Wasco, W., Poorkaj, P., Romano, D.M., Oshima, J., Pettingell, W.H., Yu, C.E., Jondro, P.D., Schmidt, S.D., Wang, K., et al. (1995). Candidate gene for the chromosome 1 familial Alzheimer's disease locus. Science 269, 973–977.

Liu, P., Jenkins, N.A., and Copeland, N.G. (2003). A highly efficient recombineering-based method for generating conditional knockout mutations. Genome Res 13, 476–484.

Matevossian, A., and Akbarian, S. (2008). A chromatin assay for human brain tissue. J Vis Exp.

Minster, R.L., Demirci, F.Y., DeKosky, S.T., and Kamboh, M.I. (2009). No association between CALHM1 variation and risk of Alzheimer disease. Hum Mutat 30, E566–569.

Moyer, B.D., Hevezi, P., Gao, N., Lu, M., Kalabat, D., Soto, H., Echeverri, F., Laita, B., Yeh, S.A., Zoller, M., et al. (2009). Expression of genes encoding multi-transmembrane proteins in specific primate taste cell populations. PLoS One 4, e7682.

Nacmias, B., Tedde, A., Bagnoli, S., Lucenteforte, E., Cellini, E., Piaceri, I., Guarnieri, B.M., Bessi, V., Bracco, L., and Sorbi, S. (2010). Lack of implication for CALHM1 P86L common variation in Italian patients with early and late onset Alzheimer's disease. J Alzheimers Dis 20, 37–41.

Piedrahita, J.A., Zhang, S.H., Hagaman, J.R., Oliver, P.M., and Maeda, N. (1992). Generation of mice carrying a mutant apolipoprotein E gene inactivated by gene targeting in embryonic stem cells. Proc Natl Acad Sci U S A 89, 4471–4475.

Rozen, S., and Skaletsky, H. (2000). Primer3 on the WWW for general users and for biologist programmers. Methods Mol Biol 132, 365–386.

Sambrook, J., and Russell, D.W. (2001). Molecular cloning: a laboratory manual, Vol 2 (CSHL press).

Saunders, A.M., Strittmatter, W.J., Schmechel, D., George-Hyslop, P.H., Pericak-Vance, M.A., Joo, S.H., Rosi, B.L., Gusella, J.F.,

Crapper-MacLachlan, D.R., Alberts, M.J., et al. (1993). Association of apolipoprotein E allele epsilon 4 with late-onset familial and sporadic Alzheimer's disease. Neurology 43, 1467–1472.

Shen, J., Bronson, R.T., Chen, D.F., Xia, W., Selkoe, D.J., and Tonegawa, S. (1997). Skeletal and CNS defects in Presenilin-1-deficient mice. Cell 89, 629–639.

Sherrington, R., Rogaev, E.I., Liang, Y., Rogaeva, E.A., Levesque, G., Ikeda, M., Chi, H., Lin, C., Li, G., Holman, K., et al. (1995). Cloning of a gene bearing missense mutations in early-onset familial Alzheimer's disease. Nature 375, 754–760.

Shibata, N., Kuerban, B., Komatsu, M., Ohnuma, T., Baba, H., and Arai, H. (2010). Genetic association between CALHM1, 2, and 3 polymorphisms and Alzheimer's disease in a Japanese population. J Alzheimers Dis 20, 417–421.

Sleegers, K., Brouwers, N., Bettens, K., Engelborghs, S., van Miegroet, H., De Deyn, P.P., and Van Broeckhoven, C. (2009). No association between CALHM1 and risk for Alzheimer dementia in a Belgian population. Hum Mutat 30, E570–574.

Tanzi, R.E. (1999). A genetic dichotomy model for the inheritance of Alzheimer's disease and common age-related disorders. J Clin Invest 104, 1175–1179.

Vorhees, C.V., and Williams, M.T. (2006). Morris water maze: procedures for assessing spatial and related forms of learning and memory. Nat Protoc 1, 848–858.

Yu, H., Saura, C.A., Choi, S.Y., Sun, L.D., Yang, X., Handler, M., Kawarabayashi, T., Younkin, L., Fedeles, B., Wilson, M.A., et al. (2001). APP processing and synaptic plasticity in presenilin-1 conditional knockout mice. Neuron 31, 713–726.

Zhang, Z., Schwartz, S., Wagner, L., and Miller, W. (2000). A greedy algorithm for aligning DNA sequences. J Comput Biol 7, 203–214.

Zheng, H., Jiang, M., Trumbauer, M.E., Sirinathsinghji, D.J., Hopkins, R., Smith, D.W., Heavens, R.P., Dawson, G.R., Boyce, S., Conner, M.W., et al. (1995). beta-Amyloid precursor protein-deficient mice show reactive gliosis and decreased locomotor activity. Cell 81, 525–531.

